

Spin-orbit potential properties derived from measurements of analyzing powers for neutron scattering from ^{54}Fe and ^{65}Cu

C. E. Floyd,* P. P. Guss,[†] R. C. Byrd, K. Murphy, and R. L. Walter
Department of Physics, Duke University, Durham, North Carolina 27706
and Triangle Universities Nuclear Laboratory, Durham, North Carolina 27706

J. P. Delaroche

Service de Physique Neutronique et Nucleaire, Centre d'Etudes de Bruyeres-le-Chatel, 92542 Montrouge, Cedex, France
 (Received 20 May 1983)

Angular distributions of the analyzing power $A_y(\Theta)$ have been measured for elastic scattering of neutrons from ^{54}Fe and ^{65}Cu at 10 and 14 MeV and for inelastic scattering to the first 2^+ state of ^{54}Fe at 10 MeV. We have combined the results with previous measurements and analyses of the differential cross sections in the same energy range and have carried out new deformed optical model calculations where the major concern was to study the spin-orbit interaction. The need for an imaginary spin-orbit term $W_{\text{SO}}(r)$ is discussed. The (n, n') data are important in reducing an ambiguity found between the deformation β_{SO} of the real spin-orbit potential and the strength W_{SO} of the imaginary spin-orbit potential.

NUCLEAR REACTIONS $^{54}\text{Fe}, ^{65}\text{Cu}(n,n), E=10, 14$ MeV; $^{54}\text{Fe}(n,n'), E=10$ MeV. Measured $A_y(E, \theta)$. Deduced deformed complex spin-orbit potentials. Coupled channels calculations.

I. INTRODUCTION

Most of the polarization information accumulated over the years for investigating the spin-orbit (SO) part of the nucleon-nucleus optical potential has been obtained through proton scattering measurements at incident energies E_p between 15 MeV and 1 GeV. To date, the SO potentials used in neutron-nucleus scattering calculations have usually been based primarily on these proton polarization results. Two such SO potentials that have been popular for neutrons are those of Perey¹ and of Becchetti and Greenlees.² On the other hand, not much specific information about the SO potential for neutrons has been learned directly from neutron scattering cross-section measurements. In fact, accurate experiments with polarized neutron beams have been very difficult to perform at energies sufficiently high that the direct reaction mechanism dominates.

In the present paper we report the first in a series of experiments and analyses conducted at the Triangle Universities Nuclear Laboratory (TUNL) which involve the scattering of polarized neutrons from medium- and heavy-mass nuclei at incident energies between 8 and 18 MeV. The aim of this program is to *directly* determine the properties of the SO potential

$$U_{\text{SO}}(r) = V_{\text{SO}}(r) + iW_{\text{SO}}(r)$$

for the neutron-nucleus interaction and, more generally, to provide a test for those who are modeling the nucleon-nucleus interaction on a microscopic basis. In this paper we report $A_y(\Theta)$ measurements for neutron elastic scattering from ^{54}Fe and ^{65}Cu at 10 and 14 MeV. A preliminary

report on the data for elastic scattering was given in Ref. 3. In addition, we present here $A_y(\Theta)$ data at 10 MeV for the inelastic scattering to the 2^+ state of ^{54}Fe at 1.4 MeV.

In contrast to the proton case, for neutron interactions the availability of data such as the total cross section σ_T , s - and p -wave strength functions S_0 and S_1 , and potential radii R' place stringent constraints on the neutron optical model⁴ and thereby help to remove many of the ambiguities underlying the optical model parametrization. In earlier coupled-channels analyses⁵ of (n,n) and (n,n') cross sections for $^{54,56}\text{Fe}$ and $^{63,65}\text{Cu}$, we paid close attention to the measured values for S_0 , S_1 , R' , and σ_T . In the present work we have focused on the $A_y(\Theta)$ data, keeping in mind that the optical potentials developed here must be consistent with these earlier analyses.

In addition to determining the strength, radius, and diffuseness of $V_{\text{SO}}(r)$, the need to incorporate an imaginary term $W_{\text{SO}}(r)$ in $U_{\text{SO}}(r)$ will be discussed. The size of this term is not known for neutron scattering from medium-mass nuclei and, in fact, is also not even well determined for proton scattering below 100 MeV.⁶⁻⁸ Also, we have examined the importance of $A_y(\Theta)$ measurements for determining $W_{\text{SO}}(r)$ when the real SO potential $V_{\text{SO}}(r)$ is deformed. Furthermore, we illustrate the significance of $A_y(\Theta)$ measurements for inelastic scattering in reducing an ambiguity found between the magnitude of W_{SO} and the spin-orbit deformation parameter β_{SO} associated with $V_{\text{SO}}(r)$. The code ECIS79 (Ref. 9) of Raynal was used to perform the coupled-channels analyses presented here.

II. EXPERIMENTAL ARRANGEMENT AND DETAILS OF DATA ANALYSIS

As the techniques for performing $A_y(\Theta)$ measurements with pulsed polarized neutron beams at TUNL have been

given elsewhere,^{10,11} only a brief description and specific details of the experiment will be reported here. The source of the neutron beam is the ${}^2\text{H}(\vec{d}, \vec{n}){}^3\text{He}$ reaction at the reaction angle of 0° . This reaction, when initiated with polarized deuteron beams, produces a beam of polarized neutrons having about 90% of the vector polarization p_y of the incident deuteron beam.¹² Typically, in the present work the time-averaged deuteron beam intensity was 100 nA. The beam, which had a polarization p_y of about 0.65 and a pulse width of about 2 ns, was incident on a deuterium gas cell. The cell was 5 cm long and pressurized to 3 bars, which gave an energy spread of $\Delta E_n = 0.44$ MeV for 10 MeV neutrons ($E_d = 6.8$ MeV) and 0.29 MeV for 14 MeV neutrons ($E_d = 11.0$ MeV).

The scattering samples were comprised of enriched ${}^{54}\text{Fe}$ (97.6%) and ${}^{65}\text{Cu}$ (99.7%) and were cylindrical in shape with heights 2.4 and 3.4 cm, diameters 1.9 and 2.0 cm, and masses 50.9 and 84.6 g, respectively. The scatterers, which were located 9.3 cm from the center of the deuterium gas cell, subtended a half-angle of about 6° .

Two heavily shielded neutron detectors¹³ are used in the $A_y(\Theta)$ measurements. Both are set at equal scattering angles, and one counts neutrons scattered to the left, the other to the right. These detectors were located at flight paths of 3.7 and 2.7 m, respectively, for the elastic scattering measurements. For the ${}^{54}\text{Fe}(n, n')$ measurements at 10 MeV the flight paths were increased to 5.7 and 3.8 m, respectively, in order to resolve the elastic scattering peak from the peak for inelastic scattering to the 1.4-MeV excited state. The detectors subtended angles ranging from 2.7° to 1.0° for the two flight-path settings.

When using a "two-detector, spin-flip" technique¹⁴ in $A_y(\Theta)$ measurements, one only needs to measure ratios of the yields in the detectors; it is not necessary to normalize either to yields observed in flux-monitor detectors or to accumulated charge at the target. Nevertheless, this information was obtained as a check on the operation of the detection and electronics systems.

At each scattering angle data were obtained until the statistical accuracy in $A_y(\Theta)$ typically was about $\Delta A_y(\Theta) = \pm 0.04$. However, at forward angles, where the differential cross section $\sigma(\Theta)$ is large, the accuracy

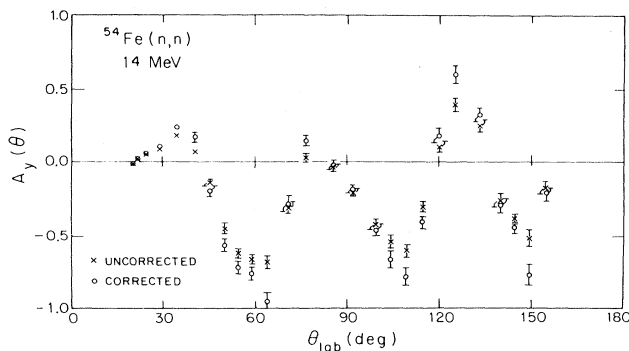


FIG. 1. $A_y(\Theta)$ measurements for ${}^{54}\text{Fe}(n, n)$ at 14 MeV. Comparison between uncorrected data and data corrected for effects due to multiple scattering, attenuation, and finite geometry.

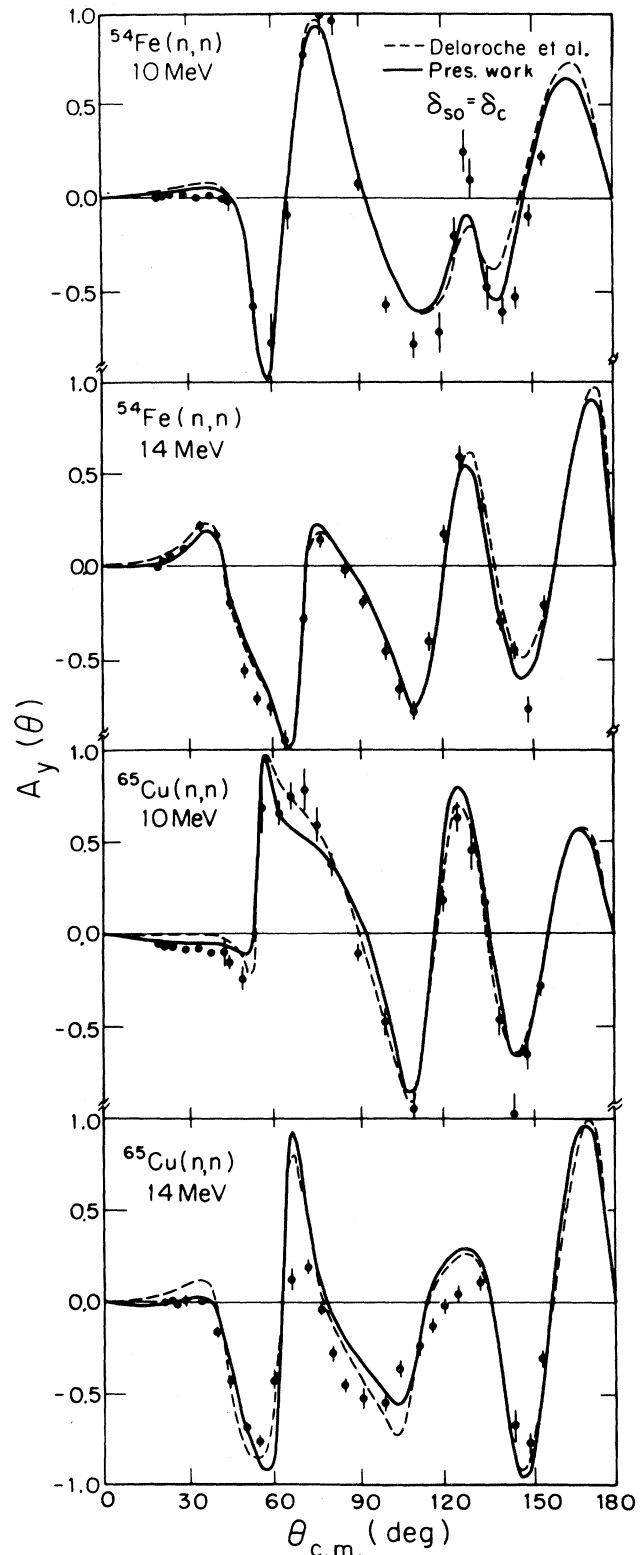


FIG. 2. Analyzing powers for neutron elastic scattering from ${}^{54}\text{Fe}$ and ${}^{65}\text{Cu}$ at 10 and 14 MeV. The dashed lines represent CC predictions using the parameters of Ref. 5. The solid lines represent CC calculations where the present spin-orbit potentials are used (see Sec. III B).

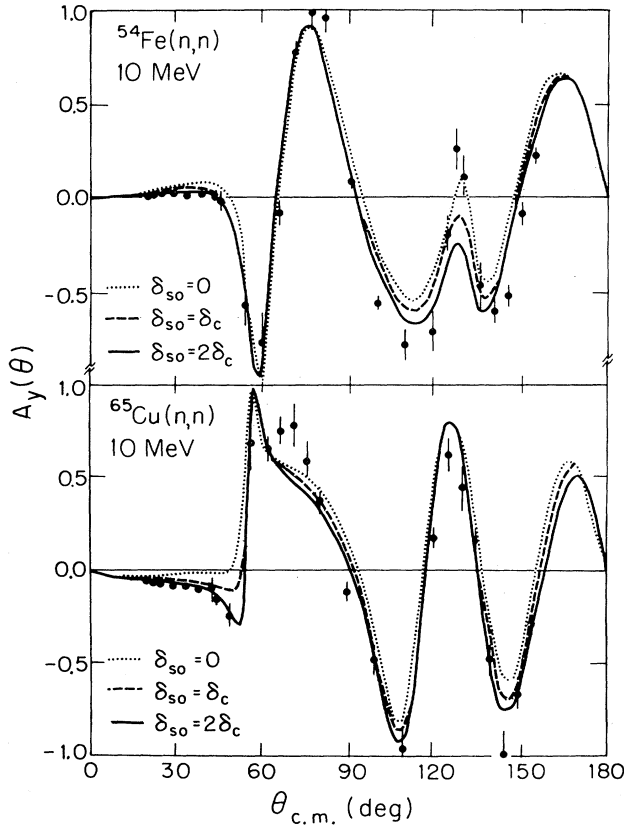


FIG. 3. Analyzing powers for elastic scattering from ^{54}Fe and ^{65}Cu at 10 MeV. Comparison between the present data and CC predictions when δ_{so} is set to 0, δ_c , and $2\delta_c$ (dotted, dashed, and solid lines, respectively).

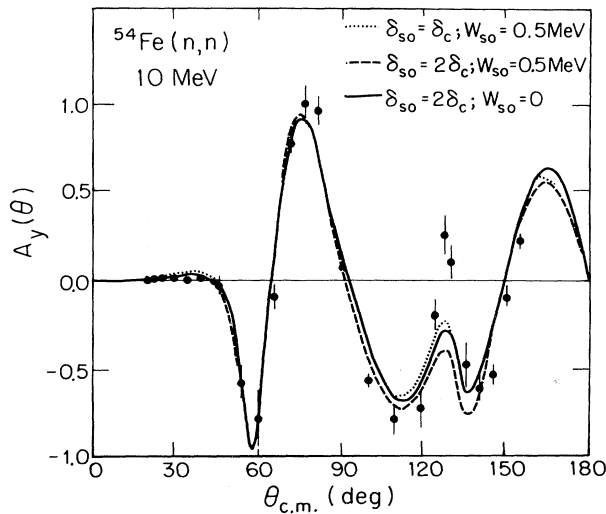


FIG. 4. Analyzing power for elastic scattering from ^{54}Fe at 10 MeV. Comparison between the measurements and CC predictions. The solid and dashed lines are for $\delta_{\text{so}}=2\delta_c$ and $W_{\text{so}}=0$ and 0.5 MeV, respectively. The dotted line is for $\delta_{\text{so}}=\delta_c$ and $W_{\text{so}}=0.5$ MeV.

achieved was $\Delta A_y(\Theta) = \pm 0.005$. For the $^{54}\text{Fe}(n,n')$ measurements the counting rate was low—about six hours was required at each angle to obtain the reported accuracy of about ± 0.06 .

Time-of-flight spectra were acquired using a DDP-224 computer, stored on magnetic tape, and reanalyzed at a later date. When analyzing the spectra, narrow windows were set on the elastic scattering peak in such a way that inelastic scattering events were eliminated.

In order to increase the counting rate, the experiment employed a tight geometrical configuration and relatively large scattering samples. The measured yields had to be corrected for attenuation, multiple scattering, and finite geometry effects. These corrections were made using the Monte Carlo code JANE developed at Tübingen and TUNL.¹⁵ In the minima of the scattering cross sections the corrections for these effects are large. A sample of the uncorrected and corrected $A_y(\Theta)$ data is shown in Fig. 1 for ^{54}Fe at 14 MeV. The final uncertainties $\Delta A_y(\Theta)$ are increased to include the additional statistical uncertainty caused by removing the events due to multiple scattering. In several cases $\Delta A_y(\Theta)$ exceeds ± 0.10 . An uncertainty in the scale factor of about ± 0.03 to account for the uncertainty in the neutron beam polarization has not been included in the error bars shown for the $A_y(\Theta)$ data. Tables of the final results for $A_y(\Theta)$ and $\Delta A_y(\Theta)$ are available from TUNL.

III. OPTICAL MODEL ANALYSES

A. Overview

The general form of the optical potential $U(\vec{r})$ which is assumed in the coupled-channels (CC) calculations may be expressed as follows:

$$\begin{aligned}
 U(\vec{r}) = & -(V + iW_V)f(r, a_V, R_V) \\
 & + 4ia_D W_D \frac{d}{dr} f(r, a_D, R_D) \\
 & - 2i\lambda_\pi^2 V_{\text{SO}} \vec{\nabla} f(r, a_{\text{SO}} R_{\text{SO}}) \times \vec{\nabla} \cdot \vec{s} \\
 & + 2i\lambda_\pi^2 W_{\text{SO}} \frac{1}{r} \frac{d}{dr} f(r, a_{W_{\text{SO}}}, R_{W_{\text{SO}}}) \vec{1} \cdot \vec{s}. \quad (1)
 \end{aligned}$$

The third term represents the full Thomas form of the spin-orbit (SO) interaction,¹⁶ that is, a deformed real SO potential, which reduces to the usual real SO potential for $\delta_{\text{so}}=0$. The last term represents an imaginary SO potential $W_{\text{SO}}(r)$, which is spherical throughout the present work. The form factor $f(r, a_i, R_i)$ is of a Woods-Saxon type,

$$f(r, a_i, R_i) = \left[1 + \exp \left(\frac{r - R_i}{a_i} \right) \right]^{-1},$$

where R_i is expressed in the center-of-mass system as

$$R_i = r_i A^{1/3} \left[1 + \sum_{\mu} \alpha_{2\mu}^i Y_2^{\mu}(\Omega) \right]$$

for a collective nucleus having quadrupole surface vibrations. The $\alpha_{2\mu}^i$ values can be related to the deformation lengths $\delta_i = \beta_{2i}^i r_i A^{1/3}$. Complex coupling form factors

were assumed for the central parts of $U(\vec{r})$. Deformation lengths δ_c of the central potential were constrained to have identical values for both real and imaginary terms. Eventually, the deformation length δ_{SO} for the spin-orbit potential was varied from the identity $\delta_{SO}=\delta_c$ assumed in Ref. 5. In the present calculations it was found that the data could be described adequately without the inclusion of a volume absorption term; therefore W_V was set to zero.

In preparing a data set to compare with the CC calculations, consideration was given to the Mott-Schwinger (MS) interaction, that is, the interaction of the magnetic moment of the neutron which is moving in the electromagnetic field of the nucleus. This interaction has a strong influence on $A_y(\Theta)$ predictions for elastic scattering at far forward angles. As the CC code does not yet include this interaction, an estimate of its effect on $A_y(\Theta)$ was made using a spherical optical model code which has been modified to include the MS potential.¹⁷ The corrections were small, amounting to a shift of less than 0.02. The elastic scattering data were shifted accordingly for the search computations and the illustrations of the present paper. No corrections for MS scattering were applied to the (n,n') data; presumably they are negligible.

The analysis of the present $A_y(\Theta)$ data is based on earlier TUNL (n,n) and (n,n') differential cross section studies^{5,13} for $^{54,56}\text{Fe}$ and $^{63,65}\text{Cu}$ at incident energies between 8 and 14 MeV. In this earlier work, which ignored the $W_{SO}(r)$ term, it was pointed out⁵ that the optical model predictions for $\sigma(\Theta)$ are sensitive enough to the parameters for the spin-orbit potential to allow one to roughly estimate the geometrical properties of $V_{SO}(r)$. We have used the parameters of Ref. 5 to predict $A_y(\Theta)$ for elastic and inelastic scattering. These CC calculations are shown as dashed lines together with the present elastic scattering measurements for ^{54}Fe and ^{65}Cu in Fig. 2. As can be seen, the gross structures in the $A_y(\Theta)$ distributions are reasonably well reproduced. However, the achievement of better fits requires a fine tuning of the spin-orbit potential pa-

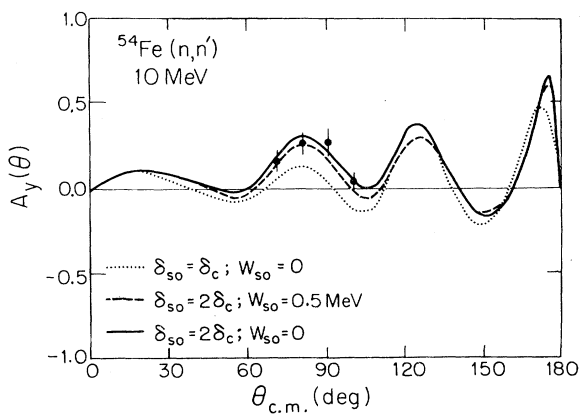


FIG. 5. Analyzing power data at 10 MeV for inelastic scattering to the first 2^+ state of ^{54}Fe . The solid and dashed lines represent CC predictions for $\delta_{SO}=2\delta_c$ and $W_{SO}=0$ and 0.5 MeV, respectively. The dotted line is for $\delta_{SO}=\delta_c$ and $W_{SO}=0$.

rameters V_{SO} , a_{SO} , and r_{SO} . In particular, the high counting rates at forward angles permit $A_y(\Theta)$ to be measured very accurately, i.e., to better than ± 0.01 , and the calculations indicated by the dashed curves in Fig. 2 significantly disagree with the data in three out of the four instances shown.

B. Analyzing powers for elastic scattering

The search for better spin-orbit potentials has been performed independently for ^{54}Fe and ^{65}Cu , keeping unchanged the central terms of the potentials of Ref. 5. The spin-orbit potentials have been varied only slightly; we have verified that this procedure preserves the fits of Ref. 5 to the differential cross sections. In the CC calculations, we have proceeded as follows for each nucleus: (i) The best fits for $A_y(\Theta)$ were sought at 10 and 14 MeV, independently; (ii) the best-fit parameters V_{SO} , a_{SO} , and r_{SO} obtained at each energy were combined to produce a set of average parameters. The results were $V_{SO}=5.30$ MeV and $a_{SO}=0.464$ fm for both nuclei; the values of r_{SO} were 1.040 fm for ^{54}Fe and 1.110 fm for ^{65}Cu . The main difference between these SO parameters and those found in our previous work (see Table 1 and Table 5 of Refs. 5 and 13, respectively) are a smaller strength V_{SO} and a smaller diffuseness a_{SO} for the present work. Moreover, a_{SO} has a value significantly smaller than the 0.75 fm result obtained in the spherical optical model analysis of Becchetti and Greenlees,² which is sometimes used in neutron scattering analyses.¹⁸ Our parameter set is closer to the older set recommended¹ by Perey for protons ($V_{SO}=6.0$ MeV, $r_{SO}=1.12$ fm, and $a_{SO}=0.47$ fm). The new predictions for $A_y(\Theta)$ are shown as solid lines in Fig. 2. These calculations are in much better agreement with the high-accuracy data at forward angles, particularly for ^{65}Cu , where the χ^2 for the $A_y(\Theta)$ fit is reduced by more than a factor of 3.

In the CC calculations of Ref. 5 it was assumed that $\delta_{SO}=\delta_c$. This equality, chosen somewhat arbitrarily, seemed reasonable from what was known from previous (p,p') scattering studies.¹⁹ Using the parameters V_{SO} , a_{SO} , and r_{SO} obtained above, we have carried out new CC calculations which allow δ_{SO} to depart from δ_c . The $A_y(\Theta)$ measurements at 10 MeV are shown in Fig. 3 together with CC predictions for δ_{SO} values set to 0, δ_c , and $2\delta_c$, successively. It can be seen that the predictions are rather sensitive to the value assumed for δ_{SO} . When δ_{SO} is increased, the predicted $A_y(\Theta)$ distributions are pushed downward. These findings, which are also seen at 14 MeV, seem to be *specific to the neutron elastic analyzing powers*: at comparable incident energies the corresponding sensitivity calculations made for *proton elastic scattering analyzing powers* do not show the same effects (see Refs. 5 and 20).

On the basis of these CC calculations carried out for neutron analyzing powers for *elastic scattering*, it is doubtful that a unique value of δ_{SO} can be determined. In order to illustrate this point, we have performed further CC calculations in which the complete Eq. (1) for the potential is assumed; that is, an imaginary SO potential $W_{SO}(r)$ is now included. According to Brieva and Rook,⁷ the radius $r_{W_{SO}}$ should be larger than r_{SO} ; thus, we have initially

chosen $r_{W_{SO}} = 1.03r_{SO}$. Furthermore, $a_{W_{SO}}$ was set identical to a_{SO} in order to reduce the number of free parameters. Employing all these conditions, values for δ_{SO} ranging from 0 to $2\delta_c$ were chosen, and W_{SO} was varied to obtain the best description of the data. The depth W_{SO} was the only free parameter for $W_{SO}(r)$, once the value of δ_{SO} was chosen. One result is that within this range for δ_{SO} , W_{SO} reaches positive values which might be as large as $+1.0$ MeV. We have verified that this value does not change much when $r_{W_{SO}}$ and $a_{W_{SO}}$ are varied slightly from the respective values assumed for them above. A positive W_{SO} value of 1.0 MeV is at variance with the microscopic model predictions of Brieva and Rook⁷ for proton scattering above 20 MeV. Their potential depth W_{SO} has the opposite sign and a smaller strength than that found here. On the other hand, the energy dependence of W_{SO} at lower energies is not addressed in the work of Brieva and Rook, nor have previous experiments determined W_{SO} values in our energy range for the Fe-Cu mass region. Although we recently reported²¹ a W_{SO} value with a similar sign and magnitude for $^{208}\text{Pb}(\bar{n},n)$ scattering at 10 MeV, we hasten to add that the present Fe-Cu analysis does not provide conclusive evidence for the need of a $W_{SO} \neq 0$.

In addition, another result is that the values found here for W_{SO} depend strongly on the value assumed for δ_{SO} . An increase of δ_{SO} can be compensated by an appropriate increase of W_{SO} when fitting $A_y(\Theta)$. The ambiguity between δ_{SO} and W_{SO} makes it impossible to determine properly either parameter using only $A_y(\Theta)$ and $\sigma(\Theta)$ measurements for neutron elastic scattering. This result is illustrated in Fig. 4 for ^{54}Fe at 10 MeV. Similar results were obtained for ^{54}Fe at 14 MeV, and also at both energies for ^{65}Cu .

C. Analyzing power for inelastic scattering from ^{54}Fe

The ambiguities found between δ_{SO} and W_{SO} may be resolved to some extent when $A_y(\Theta)$ measurements for inelastic scattering are also considered in the CC analysis. In our previous paper,²² we illustrated the strong sensitivity of $A_y(\Theta)$ predictions for (n,n') scattering from five nuclei to the size of the deformation length δ_{SO} . The $^{54}\text{Fe}(n,n')^{54}\text{Fe}(2^+)$ data shown in Ref. 22 were obtained as a part of the present measurements. These data are presented in Fig. 5 along with CC calculations (solid line) which assume $\delta_{SO} = 2\delta_c$ and $W_{SO} = 0$. The sensitivity to δ_{SO} is indicated by the dotted line, which corresponds to $\delta_{SO} = \delta_c$ and $W_{SO} = 0$. The solid line gives a good description of the data, and the sensitivity permits us to establish²² that, at 10 MeV, $\delta_{SO}/\delta_c = 2.0 \pm 0.4$ when W_{SO} is set to zero. Note that the solid line in Fig. 4, which gives a good representation of the elastic scattering data, also corresponds to $\delta_{SO} = 2\delta_c$ and $W_{SO} = 0$.

Finally, we relaxed the constraint that $W_{SO} = 0$ and searched for better fits simultaneously for the elastic and inelastic scattering data, allowing the code to search on W_{SO} while keeping $\delta_{SO} = 2\delta_c$. The best value was found to be $W_{SO} \sim +0.5$ MeV. These new calculations are shown as dashed lines in Figs. 4 and 5. There is a little

improvement for the elastic scattering when comparing the dashed and solid lines in Fig. 4. For inelastic scattering both solid and dashed lines agree with the measurements.

IV. SUMMARY AND CONCLUSIONS

Analyzing power measurements for elastic scattering of neutrons from ^{54}Fe and ^{65}Cu at 10 and 14 MeV have been obtained at TUNL with a unique time-of-flight system. The first $A_y(\Theta)$ measurements for (n,n') scattering for a medium-mass nuclei are also reported.

In this limited range of mass and incident energy, new information on the neutron spin-orbit potential has been obtained using the CC formalism. First, it is found that the a_{SO} and V_{SO} values are significantly smaller than those deduced by Becchetti and Greenlees from global analyses. Implications from this result might be important. For instance, when only differential cross section measurements are considered in an optical model analysis, inaccurate assumptions on the spin-orbit potential parameters may lead to an improper determination of the central parts of the optical potential.

Second, it is found that the predicted $A_y(\Theta)$ values for both elastic and inelastic scattering depend on the strength of $W_{SO}(r)$ and the deformation of $V_{SO}(r)$. There is evidence for an ambiguity between the magnitudes of W_{SO} and δ_{SO} ; this ambiguity cannot be removed by considering $A_y(\Theta)$ measurements for elastic scattering only. For instance, comparable fits to the elastic scattering data for both ^{54}Fe and ^{65}Cu can be obtained using $\delta_{SO} = 0$ and $W_{SO} = +1$ MeV, $\delta_{SO} = \delta_c$ and $W_{SO} = +0.5$ MeV, or $\delta_{SO} = 2\delta_c$ and $W_{SO} = 0$. Note that, whatever magnitude W_{SO} has in the range from 0 to $+1$ MeV, the sign of $W_{SO}(r)$ is opposite to that predicted by Brieva and Rook⁷ for low incident nucleon energies.

However, if $A_y(\Theta)$ data for elastic and inelastic scattering are considered simultaneously, part of this ambiguity can be resolved. For instance, the values $\delta_{SO} = 2\delta_c$ and $W_{SO} = 0$ lead to good fits for all the $A_y(\Theta)$ measurements shown here at 10 MeV for ^{54}Fe . Since good fits were also obtained using $\delta_{SO} = 2\delta_c$ and values of W_{SO} up to $\sim +0.5$ MeV, the value of W_{SO} is estimated to be between 0 and $\sim +0.5$ MeV. The inclusion of the $A_y(\Theta)$ measurements for (n,n') scattering therefore restricts the maximum strength for W_{SO} to a value smaller than that obtained from the above analysis of the elastic scattering data only. The presently available $A_y(\Theta)$ data for neutron elastic and inelastic scattering from ^{54}Fe therefore suggest that the size of the ratio W_{SO}/V_{SO} is indeed between 0 and 0.1. The lower limit is consistent with the result predicted by Brieva and Rook⁷ for proton scattering above 20 MeV. However, the value which gave us the best fit, i.e., $W_{SO}/V_{SO} = +0.1$, is still opposite in sign to the result predicted in Ref. 7.

As a concluding remark, one might say that these findings about W_{SO} are somewhat tentative since they are based on the analysis of $A_y(\Theta)$ measurements over a limited range of energies. More $A_y(\Theta)$ data for elastic and in-

elastic scattering at higher neutron energies are required to remove the ambiguity that we found and also to establish whether W_{SO} or δ_{SO} are strongly energy dependent. Such experiments will be difficult and time consuming, but we are moving in this direction at TUNL by reducing back-

ground contributions and narrowing the width of the beam pulse.

This work was supported in part by the United States Department of Energy.

*Present address: Department of Radiology, Duke University Medical Center, Durham, NC 27710.

†Present address: Department of Physics, The College of William and Mary, Williamsburg, VA 23185.

¹F. G. Perey, in *Proceedings of the 2nd International Symposium on Polarization Phenomena of Nucleons, Karlsruhe, 1965*, edited by P. Huber and H. Schopper (Birkhäuser, Stuttgart, 1966), p. 191.

²F. D. Becchetti and G. W. Greenlees, *Phys. Rev.* **182**, 1190 (1969).

³C. E. Floyd, P. P. Guss, K. Murphy, R. C. Byrd, G. Tungate, R. L. Walter, and T. B. Clegg, *Phys. Rev. Lett.* **47**, 1042 (1981); C. E. Floyd, P. P. Guss, K. Murphy, R. C. Byrd, S. A. Wender, R. L. Walter, and T. B. Clegg, in *Polarization Phenomena in Nuclear Physics—1980 (Fifth International Symposium, Santa Fe)*, Proceedings of the Fifth International Symposium on Polarization Phenomena in Nuclear Physics, AIP Conf. Proc. No. 69, edited by G. G. Ohlsen, R. E. Brown, N. Jarmie, W. W. McNaughton, and G. M. Hale (AIP, New York, 1981), p. 398.

⁴J. P. Delaroche, Ch. Lagrange, and J. Salvy, in *Nuclear Theory in Neutron Nuclear Data Evaluation*, IAEA Report IAEA-150, 1976, Vol. II, p. 251.

⁵J. P. Delaroche, S. M. El-Kadi, P. P. Guss, C. E. Floyd, and R. L. Walter, *Nucl. Phys.* **A390**, 541 (1982).

⁶W. T. H. van Oers and J. M. Cameron, *Phys. Rev.* **184**, 1061 (1969); W. T. H. van Oers, *Phys. Rev. C* **3**, 1550 (1971); W. T. H. van Oers, Huang Haw, N. E. Davison, A. Ingemarsson, B. Fagerstrom, and G. Tibell, *Phys. Rev. C* **10**, 307 (1974).

⁷F. A. Brieva and J. R. Rook, *Nucl. Phys.* **A297**, 206 (1978).

⁸R. S. MacKintosh and A. M. Kobos, *J. Phys. G* **4**, L135 (1978).

⁹J. Raynal, code ECIS79 (unpublished).

¹⁰S. A. Wender, C. E. Floyd, T. B. Clegg, and W. R. Wylie, *Nucl. Instrum. Methods* **174**, 341 (1980); C. R. Howell and R. L. Walter, *IEEE Trans. Nucl. Sci.* **NS-30**, 1132 (1983).

¹¹W. Tornow, E. Woye, G. Mack, C. E. Floyd, K. Murphy, P. P. Guss, S. A. Wender, R. C. Byrd, R. L. Walter, T. B. Clegg, and H. Leeb, *Nucl. Phys.* **A385**, 373 (1982).

¹²P. W. Lisowski, R. L. Walter, C. E. Busch, and T. B. Clegg, *Nucl. Phys.* **A242**, 298 (1975).

¹³S. M. El-Kadi, C. E. Nelson, F. O. Purser, R. L. Walter, A. Beyerle, C. R. Gould, and L. W. Seagondollar, *Nucl. Phys.* **A390**, 509 (1982).

¹⁴G. G. Ohlsen and P. W. Keaton, Jr., *Nucl. Instrum. Methods* **109**, 41 (1973).

¹⁵E. Woye, W. Tornow, G. Mack, C. E. Floyd, P. P. Guss, K. Murphy, R. C. Byrd, S. A. Wender, R. L. Walter, T. B. Clegg, and W. Wylie, *Nucl. Phys.* **A394**, 139 (1983).

¹⁶H. Sherif and J. S. Blair, *Phys. Lett.* **26B**, 489 (1968).

¹⁷C. E. Floyd, R. L. Walter, and R. Seyler (unpublished).

¹⁸J. Rapaport, K. Kulkarni, and R. W. Finlay, *Nucl. Phys.* **A330**, 15 (1979).

¹⁹J. Raynal, in *The Structure of Nuclei*, IAEA Report IAEA-SMR-8/8, 1972, p. 75.

²⁰P. J. van Hall, J. P. M. G. Melssen, S. D. Wassenaar, O. J. Poppema, S. S. Klein, and G. J. Nijgh, *Nucl. Phys.* **A291**, 63 (1977).

²¹J. P. Delaroche, C. E. Floyd, P. P. Guss, R. C. Byrd, K. Murphy, G. Tungate, and R. L. Walter, *Phys. Rev. C* **28**, 1410 (1983).

²²P. P. Guss, C. E. Floyd, K. Murphy, C. R. Howell, R. S. Pedroni, G. M. Honore, H. G. Pfitzner, G. Tungate, R. C. Byrd, R. L. Walter, and J. P. Delaroche, *Phys. Rev. C* **25**, 2854 (1982).